Ising and Potts models in a random field: results from (quasi-)exact algorithms

Martin Weigel

Institut für Physik, Technische Universität Chemnitz, Germany

with Manoj Kumar (Coventry/Chemnitz), Ravinder Kumar (Coventry/Leipzig), Nikolaos Fytas and Argyro Mainou (Coventry), Varsha Banerjee (IIT Delhi), Sanjay Puri (JNU), Wolfhard Janke (Leipzig)

Kolloquium Theoretische Physik
Carl von Ossietzky-Universität Oldenburg, January 12, 2023

TECHNISCHE UNIVERSITÄT
IN DER KULTURHAUPTSTADT EUROPAS
CHEMNITZ

Phases of matter

Classical physics

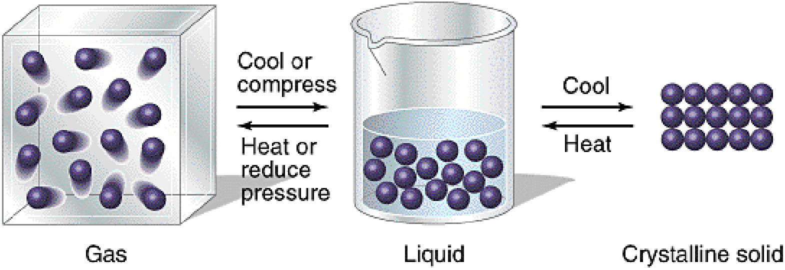

Starting point: the (2D) Ising model

Simple model for liquid-gas or magnetic transition, the Ising model.

Starting point: the (2D) Ising model

Simple model for liquid-gas or magnetic transition, the Ising model.

Hamiltonian

$$\mathcal{H} = -J \sum_{\langle i,j \rangle} s_i s_j, \quad s_i = \pm 1$$

Starting point: the (2D) Ising model

Simple model for liquid-gas or magnetic transition, the Ising model.

Hamiltonian

$$\mathcal{H} = -J \sum_{\langle i,j \rangle} s_i s_j, \quad s_i = \pm 1$$

$T \gg T_c$ $\quad$ $T \approx T_c$ $\quad$ $T \ll T_c$

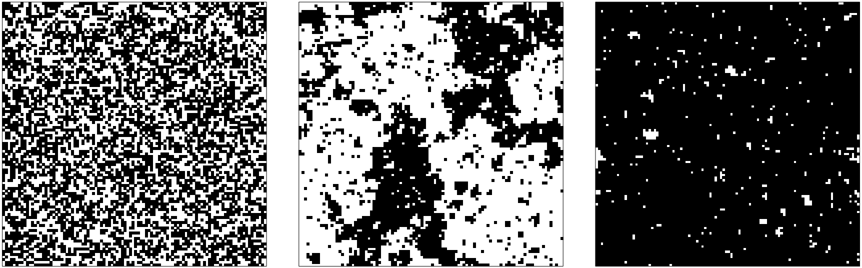

Phases of matter

Classical physics

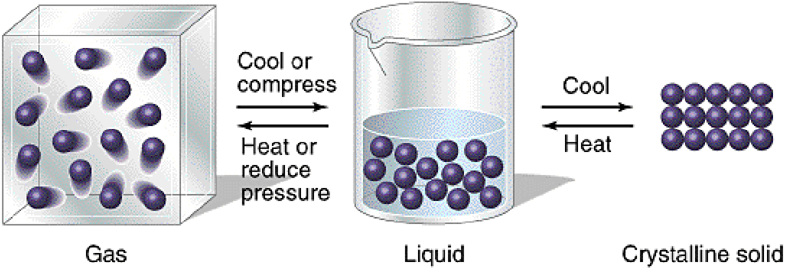

New states of matter:

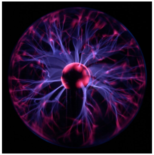

Plasma

Phases of matter

Classical physics

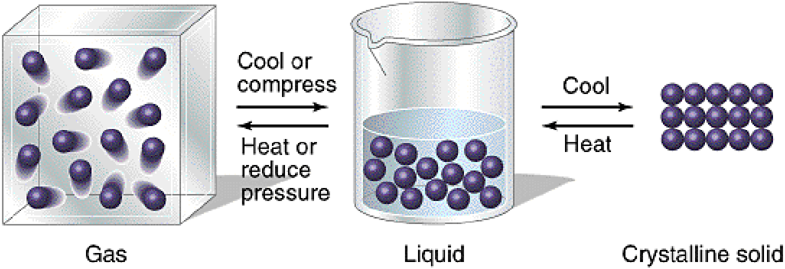

New states of matter:

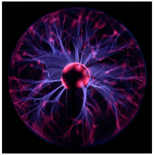

Plasma

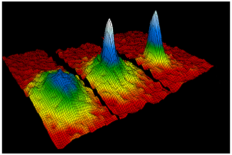

Bose-Einstein condensate

Phases of matter

Classical physics

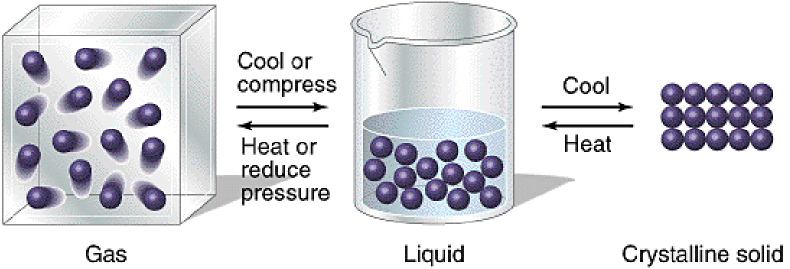

New states of matter:

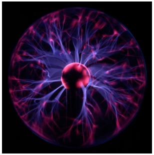

Plasma

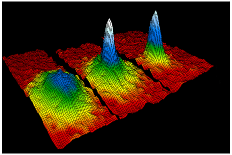

Bose-Einstein condensate

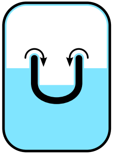

Superfluid

Phases of matter

Classical physics

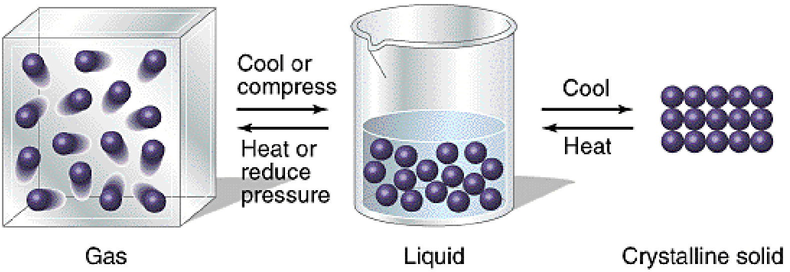

New states of matter:

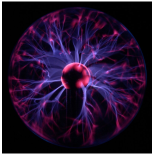

Plasma

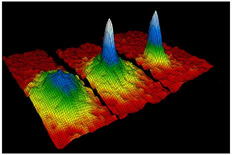

Bose-Einstein condensate

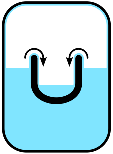

Superfluid

Glass

Phases of matter

Classical physics

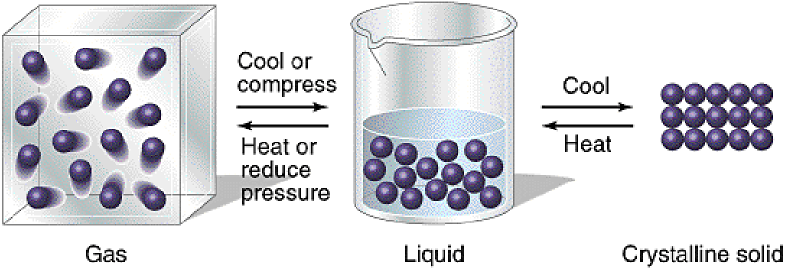

New states of matter:

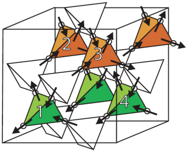

Spin ice

Phases of matter

Classical physics

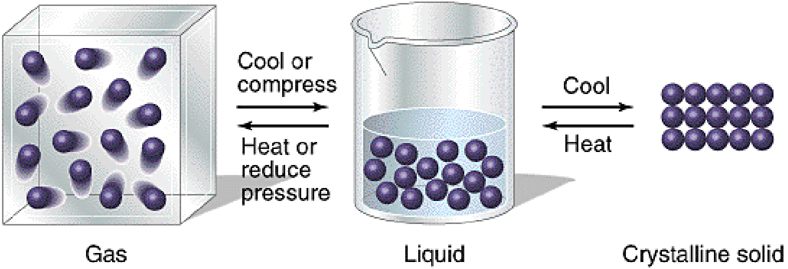

New states of matter:

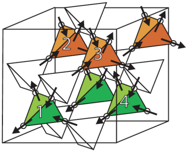

Spin ice

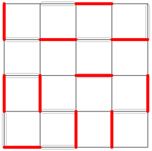

Spin liquid

Phases of matter

Classical physics

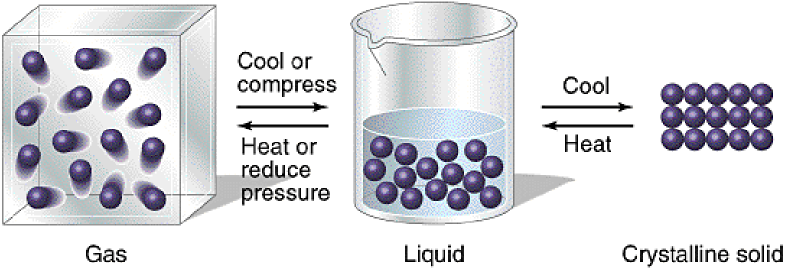

New states of matter:

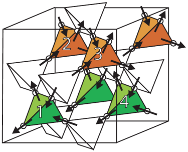

Spin ice

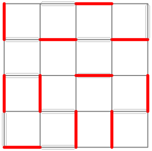

Spin liquid

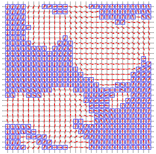

Spin glass

Phases of matter

Classical physics

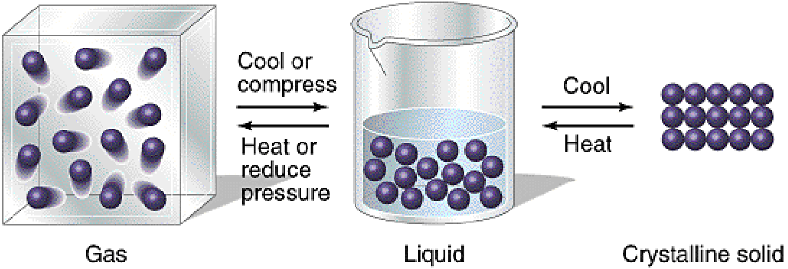

New states of matter:

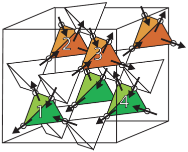

Spin ice

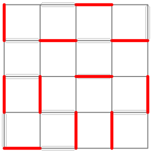

Spin liquid

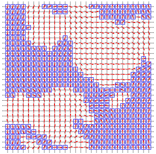

Spin glass

Disorder in condensed matter

Consider magnetic systems: **impurities** in the form of non-magnetic sites, lattice defects, random anisotropies etc. are omnipresent in laboratory samples.

Disorder in condensed matter

Consider magnetic systems: **impurities** in the form of non-magnetic sites, lattice defects, random anisotropies etc. are omnipresent in laboratory samples.

Effects on phase transitions: zoology

Disorder in condensed matter

Consider magnetic systems: **impurities** in the form of non-magnetic sites, lattice defects, random anisotropies etc. are omnipresent in laboratory samples.

Effects on phase transitions: zoology

- **Weak disorder**: long-range order is not destroyed and the nature of the ordered phase is unchanged

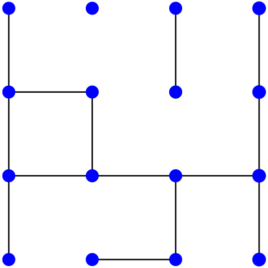

Disorder in condensed matter

Consider magnetic systems: **impurities** in the form of non-magnetic sites, lattice defects, random anisotropies etc. are omnipresent in laboratory samples.

Effects on phase transitions: zoology

- **Weak disorder**: long-range order is not destroyed and the nature of the ordered phase is unchanged
  - Disorder acting on the **energy density** (couplings): dilution, random bonds; relevance predicted by the *Harris criterion*

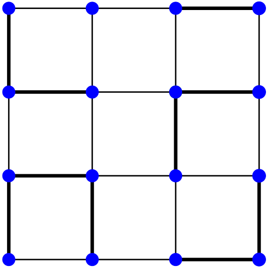

Disorder in condensed matter

Consider magnetic systems: **impurities** in the form of non-magnetic sites, lattice defects, random anisotropies etc. are omnipresent in laboratory samples.

Effects on phase transitions: zoology

- **Weak disorder**: long-range order is not destroyed and the nature of the ordered phase is unchanged
  - Disorder acting on the **energy density** (couplings): dilution, random bonds; relevance predicted by the *Harris criterion*
  - Disorder coupling to the **order parameter** (magnetization): **random fields**.

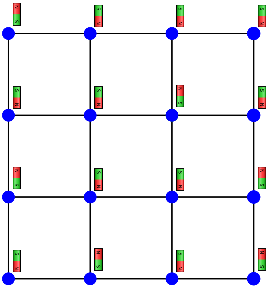

Disorder in condensed matter

Consider magnetic systems: **impurities** in the form of non-magnetic sites, lattice defects, random anisotropies etc. are omnipresent in laboratory samples.

Effects on phase transitions: zoology

- **Weak disorder**: long-range order is not destroyed and the nature of the ordered phase is unchanged
  - Disorder acting on the **energy density** (couplings): dilution, random bonds; relevance predicted by the *Harris criterion*
  - Disorder coupling to the **order parameter** (magnetization): **random fields**.
- **Strong disorder**: no long-range order, new phases of matter; typically encompasses the presence of **frustration** — **spin glasses**.

What is a spin glass?

Classical example of spin glass: noble metals weakly diluted with transition metal ions, interacting via the RKKY interaction,

$$J(\boldsymbol{R}) = J_0 \frac{\cos(2k_F R + \phi_0)}{(k_F R)^3}$$

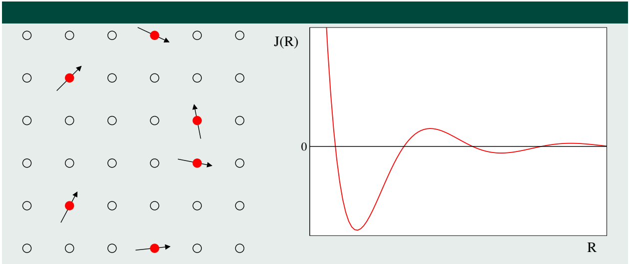

What is a spin glass?

Classical example of spin glass: noble metals weakly diluted with transition metal ions, interacting via the RKKY interaction,

$$J(\boldsymbol{R}) = J_0 \frac{\cos(2k_F R + \phi_0)}{(k_F R)^3}$$

- no long-range order down to $T = 0$
- phase transition to short-range ordered, “glassy” phase
- diverging relaxation times, memory, rejuvenation etc.

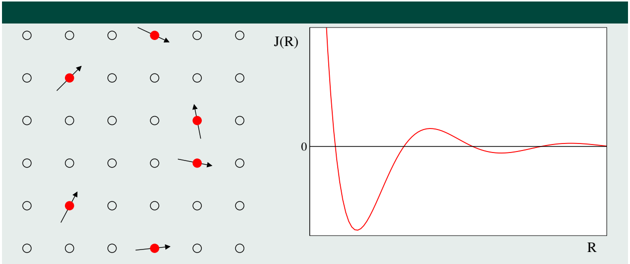

The Edwards-Anderson model

Simplify to the essential properties, **disorder** and **frustration** to yield the Edwards-Anderson (EA) model,

$$\mathcal{H} = -\frac{1}{2}\sum_{i,j} J_{ij}\, \boldsymbol{s}_i \cdot \boldsymbol{s}_j, \quad \boldsymbol{s}_i \in \mathrm{O}(n)$$

where J_{ij} are *quenched*, random variables.

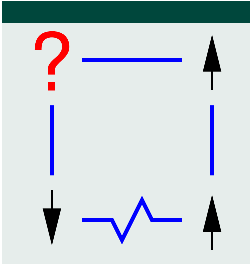

The Edwards-Anderson model

Simplify to the essential properties, **disorder** and **frustration** to yield the Edwards-Anderson (EA) model,

$$\mathcal{H} = -\frac{1}{2}\sum_{i,j} J_{ij}\, \boldsymbol{s}_i \cdot \boldsymbol{s}_j, \quad \boldsymbol{s}_i \in \mathrm{O}(n)$$

where J_{ij} are *quenched*, random variables.

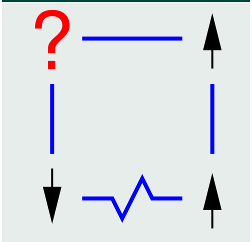

Coupling distributions

Gaussian

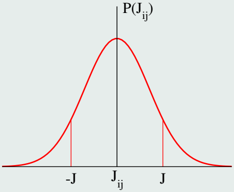

bimodal

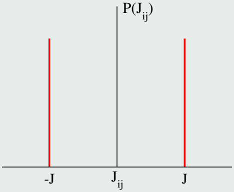

The Edwards-Anderson model

Simplify to the essential properties, **disorder** and **frustration** to yield the Edwards-Anderson (EA) model,

$$\mathcal{H} = -\frac{1}{2}\sum_{i,j} J_{ij}\, \boldsymbol{s}_i \cdot \boldsymbol{s}_j, \quad \boldsymbol{s}_i \in \mathrm{O}(n)$$

where J_{ij} are *quenched*, random variables.

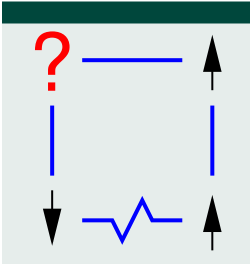

Has been investigated for $\approx$ 30 years, however no agreement on general case. Mean-field model with

$$J_{ij} = \frac{\pm 1}{\sqrt{N}},$$

known as Sherrington-Kirkpatrick (SK) model can be solved in the framework of "replica-symmetry breaking" (RSB) (Parisi *et al.*, 1979/80).

Giorgio Parisi

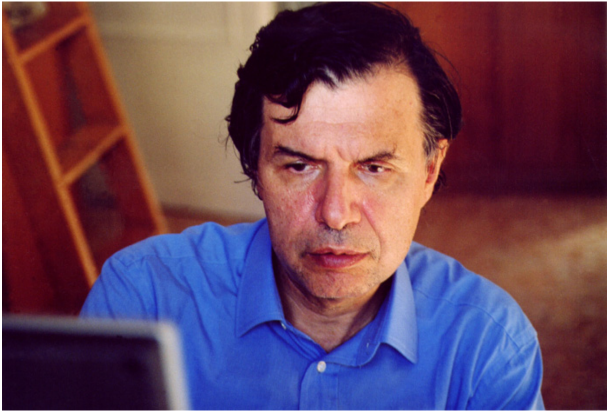

Nobel Prize 2021

The Edwards-Anderson model

Simplify to the essential properties, **disorder** and **frustration** to yield the Edwards-Anderson (EA) model,

$$\mathcal{H} = -\frac{1}{2}\sum_{i,j} J_{ij}\, \boldsymbol{s}_i \cdot \boldsymbol{s}_j, \quad \boldsymbol{s}_i \in \mathrm{O}(n)$$

where J_{ij} are *quenched*, random variables.

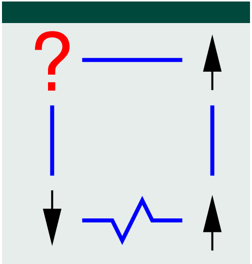

Applications

System has applications in a range of fields:

- possible role in high-T_c superconductors
- model of associative memory (Hopfield model), machine learning
- gene expression networks
- realized in D-Wave quantum computer

Ground-state calculations

At low temperatures, there are several (many) competing, **metastable** states, leading to very *slow dynamics*.

Ground-state calculations

At low temperatures, there are several (many) competing, **metastable** states, leading to very *slow dynamics*.

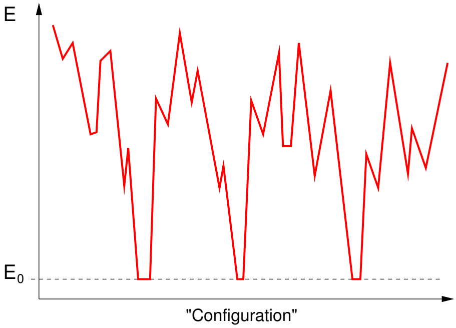

Ground-state calculations

At low temperatures, there are several (many) competing, **metastable** states, leading to very *slow dynamics*.

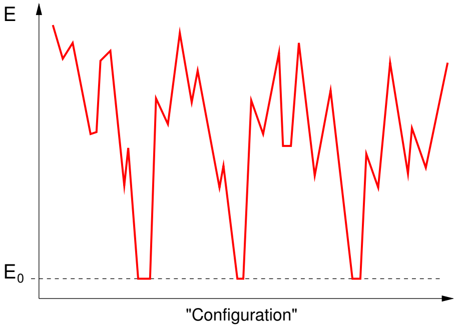

Spin-glasses and random-field systems have non-trivial states even $T = 0$. Hence much can be understood looking at **ground states**.

Ground-state calculations

At low temperatures, there are several (many) competing, **metastable** states, leading to very *slow dynamics*.

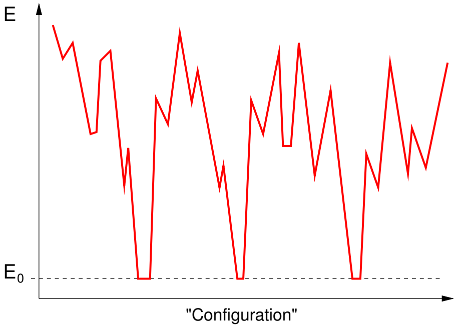

Spin-glasses and random-field systems have non-trivial states even $T = 0$. Hence much can be understood looking at **ground states**.

Finding them, however, can be difficult. In some cases it is **NP hard**.

Ising ground states as perfect matchings

System energy equals total weight of **energy strings** pairing frustrated plaquettes (Toulouse, 1977),

$$E = -\sum_{\text{strings}} |J_{ij}| + \text{const.}$$

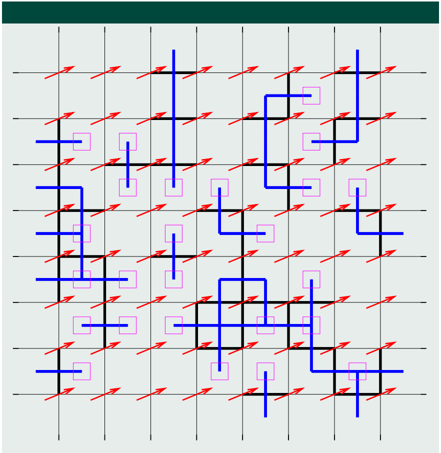

Ising ground states as perfect matchings

System energy equals total weight of **energy strings** pairing frustrated plaquettes (Toulouse, 1977),

$$E = -\sum_{\text{strings}} |J_{ij}| + \text{const.}$$

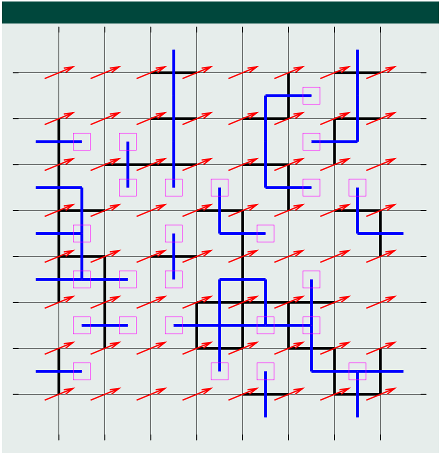

- GS search corresponds to **minimum-weight perfect matching problem** (Bieche et al., 1980)

Ising ground states as perfect matchings

System energy equals total weight of **energy strings** pairing frustrated plaquettes (Toulouse, 1977),

$$E = -\sum_{\text{strings}} |J_{ij}| + \text{const.}$$

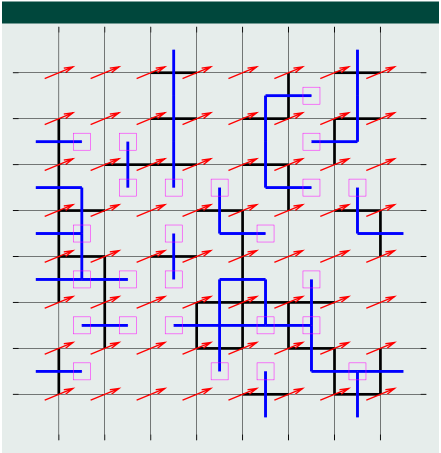

- GS search corresponds to **minimum-weight perfect matching problem** (Bieche et al., 1980)
- matching solution always corresponds to spin configuration for **planar** graphs

Ising ground states as perfect matchings

System energy equals total weight of **energy strings** pairing frustrated plaquettes (Toulouse, 1977),

$$E = -\sum_{\text{strings}} |J_{ij}| + \text{const.}$$

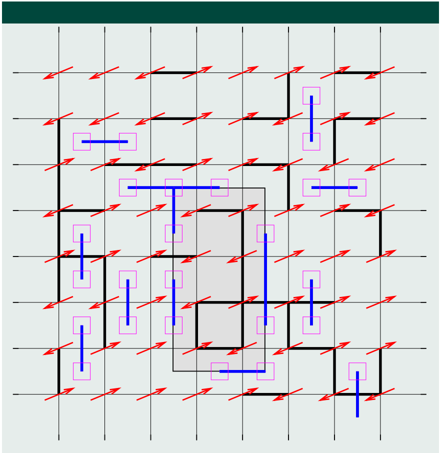

- GS search corresponds to **minimum-weight perfect matching problem** (Bieche et al., 1980)
- matching solution always corresponds to spin configuration for **planar** graphs
- can be solved in polynomial time using the “blossom” algorithm (Edmonds, 1965)

Ising ground states as perfect matchings

System energy equals total weight of **energy strings** pairing frustrated plaquettes (Toulouse, 1977),

$$E = -\sum_{\text{strings}} |J_{ij}| + \text{const.}$$

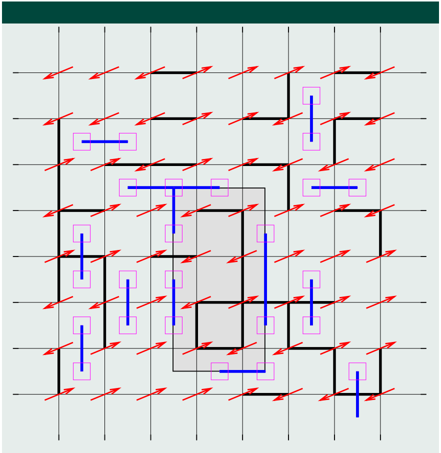

- GS search corresponds to **minimum-weight perfect matching problem** (Bieche et al., 1980)
- matching solution always corresponds to spin configuration for **planar** graphs
- can be solved in polynomial time using the "blossom" algorithm (Edmonds, 1965)
- **space complexity is O(V^2)**

Ising spin glass in 2D

Complex energy landscape leads to **slow relaxation**: sizes restricted to $L \approx 128$ (MC).

Ising spin glass in 2D

Complex energy landscape leads to **slow relaxation**: sizes restricted to $L \approx 128$ (MC).

With suitably constructed **combinatorial optimization** methods we can treat large system sizes up to $10\,000 \times 10\,000$ spins **exactly** (for $T = 0$).

Ising spin glass in 2D

Complex energy landscape leads to **slow relaxation**: sizes restricted to $L \approx 128$ (MC).

With suitably constructed **combinatorial optimization** methods we can treat large system sizes up to $10\,000 \times 10\,000$ spins **exactly** (for $T = 0$).

 $\longrightarrow$ 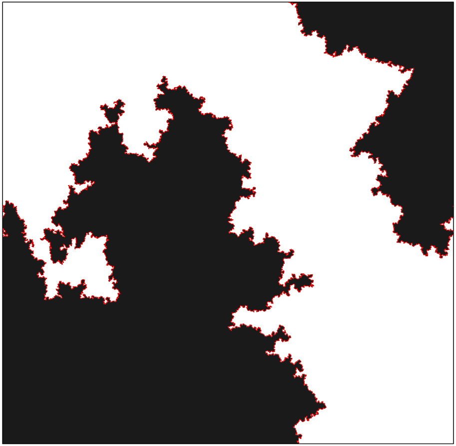

Fractal dimension

Fractal dimension of domain wall.

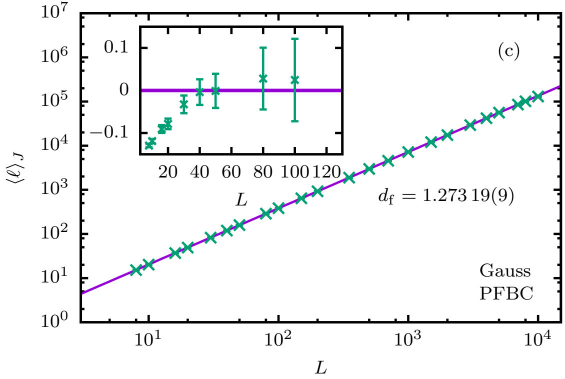

$$\langle \ell \rangle_J(L) = A_\ell L^{d_\mathrm{f}}(1 + B_\ell L^{-\omega}) + \frac{C_\ell}{L} + \frac{D_\ell}{L^2} + \cdots .$$

Results

Perform calculations for periodic-free and periodic-periodic boundary conditions.

	PFBC	PPBC
$-e_\infty$	1.3147876(7)	1.314788(3)
θ	-0.2793(3)	-0.2788(11)
d_f	1.27319(9)	1.2732(5)

Results are fully consistent with each other.

Based on SLE and further assumptions, Amoruso et al. (2006) proposed

$$d_\mathrm{f} = 1 + \frac{3}{4(3+\theta)}.$$

$d_\mathrm{f} = 1.27319(9)$ would imply $\theta = -0.2546(9)$ which is **not compatible** with the direct estimate.

Random-field Ising model

How does the behavior of the Ising model change in the presence of quenched, random fields?

Random-field Ising model

How does the behavior of the Ising model change in the presence of quenched, random fields?

$$\mathcal{H} = -J \sum_{\langle i,j \rangle} s_i s_j - \sum_i h_i s_i$$

Random-field Ising model

How does the behavior of the Ising model change in the presence of quenched, random fields?

$$\mathcal{H} = -J \sum_{\langle i,j \rangle} s_i s_j - \sum_i h_i s_i$$

h_i quenched random variables drawn, e.g., from a Gaussian,

$$h_i \sim \mathcal{N}(0, h)$$

or a bimodal distribution,

$$P(h_i) = \frac{1}{2}\delta_{h_i,-1} + \frac{1}{2}\delta_{h_i,+1}.$$

Imry and Ma argument

Is the FM phase stable?

Imry and Ma argument

Is the FM phase stable?

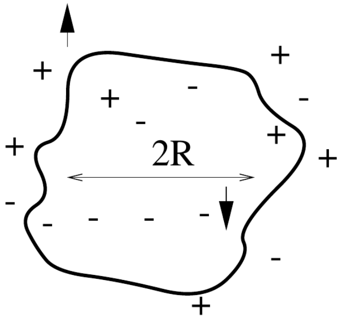

Imry and Ma argument

Is the FM phase stable?

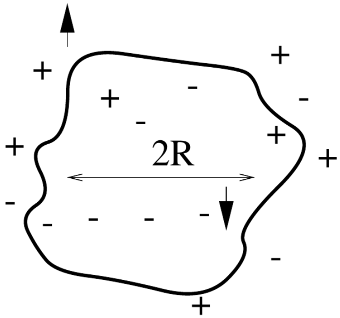

Following Imry and Ma (1975), consider a cluster of spins of (linear) size R. Overturning it will cost a surface energy of

$$E_J \sim JR^{d-1}$$

but potentially yield a gain in random-field energy of

$$E_{\mathrm{RF}} \sim hR^{d/2}$$

Imry and Ma argument (cont'd)

leading to a balance of

$$\Delta E(R) \sim JR^{d-1} - hR^{d/2}.$$

Imry and Ma argument (cont'd)

leading to a balance of

$$\Delta E(R) \sim JR^{d-1} - hR^{d/2}.$$

For large R, $\Delta E > 0$ for $d > 2$ and $\Delta E < 0$ for $d < 2$. Hence,

- FM order is stable in $d \geq 3$.
- FM order is destroyed by random fields in $d = 1$.
- $d = 2$ is marginal.

Imry and Ma argument (cont'd)

leading to a balance of

$$\Delta E(R) \sim JR^{d-1} - hR^{d/2}.$$

For large R, $\Delta E > 0$ for $d > 2$ and $\Delta E < 0$ for $d < 2$. Hence,

- FM order is stable in $d \geq 3$.
- FM order is destroyed by random fields in $d = 1$.
- $d = 2$ is marginal.

Aizenman and Wehr (1989) proved unique Gibbs state for $d \leq 2$, so no long-range order in 2D.

Domain-wall roughness

Binder (1983) considered the energy balance for a domain-wall, comparing the interface energy $2JL$ and the gain in field energy, ΔU.

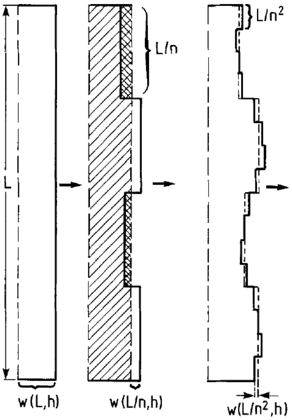

Taking the interface roughness into account, he finds

$$\Delta U \sim -(h^2/J) L \ln L / \ln n,$$

where n denotes the scale of resolution for the interface.

$U = 2JL - \Delta U$ changes sign at length scale

$$L_b \sim \exp[c(J/h)^2].$$

L_b is known as **breakup length**.

Renormalization group

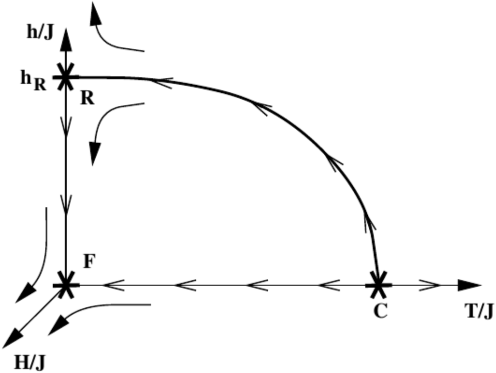

Renormalization group

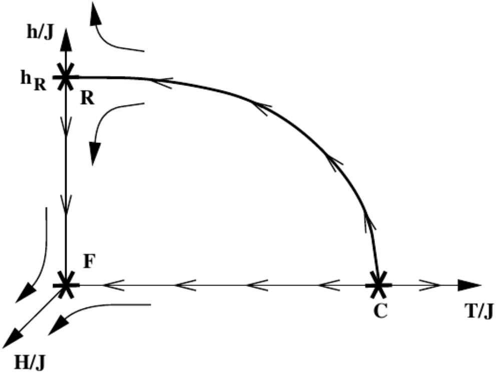

The critical behavior of the RFIM can be studied at $T = 0$, i.e., from ground states!

Renormalization group

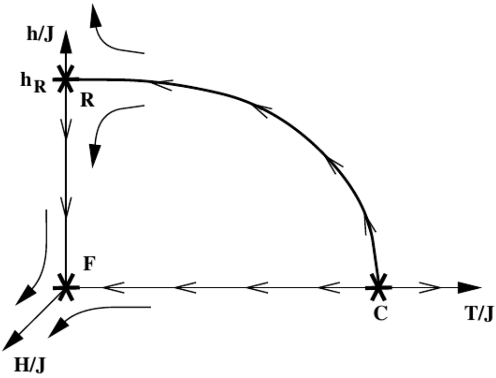

The critical behavior of the RFIM can be studied at $T = 0$, i.e., from ground states!

Renormalization group flow equation for $w = h/J$ (Bray and Moore, 1985),

$$\mathrm{d}w/\mathrm{d}l = -(\epsilon/2)w + Aw^3.$$

Break-up length

Sample ground-state configurations for $L = 512$.

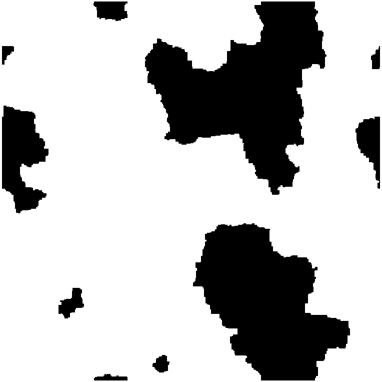

$h = 0.6$

Break-up length

Sample ground-state configurations for $L = 512$.

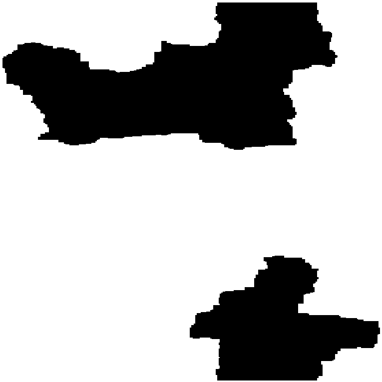

$h = 0.7$

Break-up length

Sample ground-state configurations for $L = 512$.

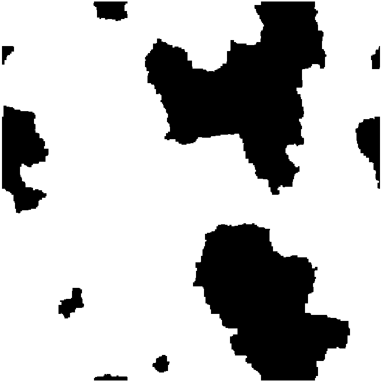

$h = 0.8$

Break-up length

Sample ground-state configurations for $L = 512$.

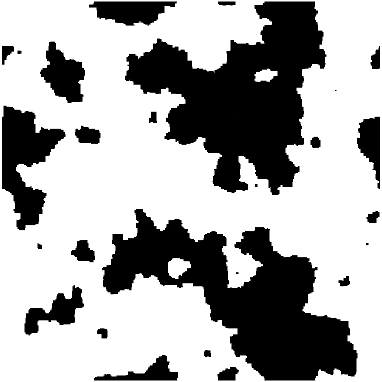

$h = 0.9$

Break-up length

Sample ground-state configurations for $L = 512$.

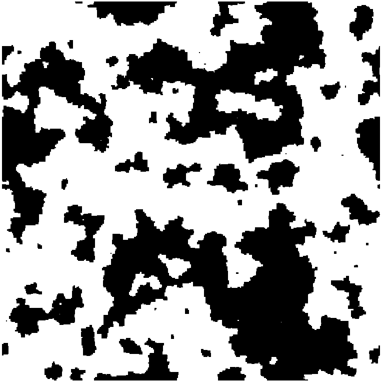

$h = 1.0$

Break-up length

Sample ground-state configurations for $L = 512$.

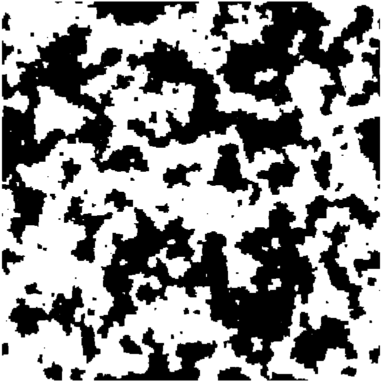

$h = 1.1$

Break-up length

Sample ground-state configurations for $L = 512$.

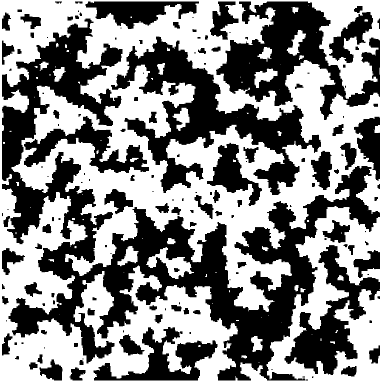

$h = 1.2$

Break-up length

Sample ground-state configurations for $L = 512$.

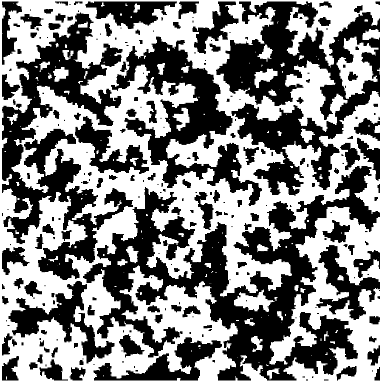

$h = 1.3$

Break-up length (cont'd)

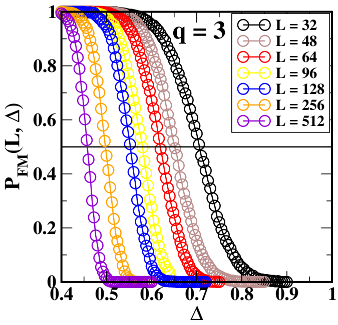

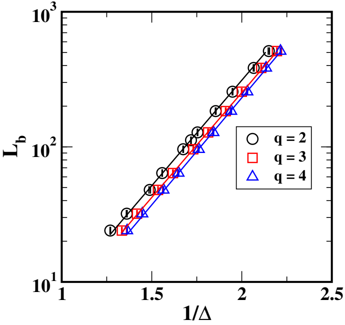

Break-up length (cont'd)

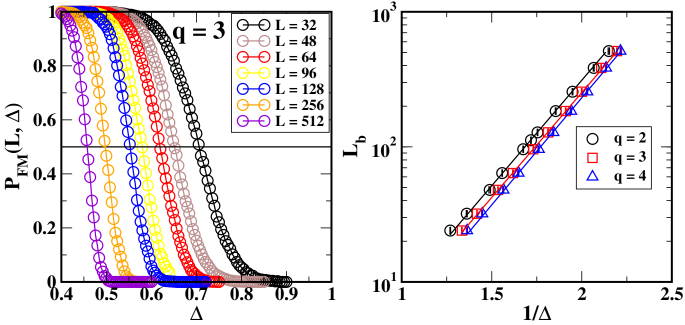

Define L_b as system size such that 50% of disorder samples at given h are FM (Seppälä et al., 1998).

Break-up length (cont'd)

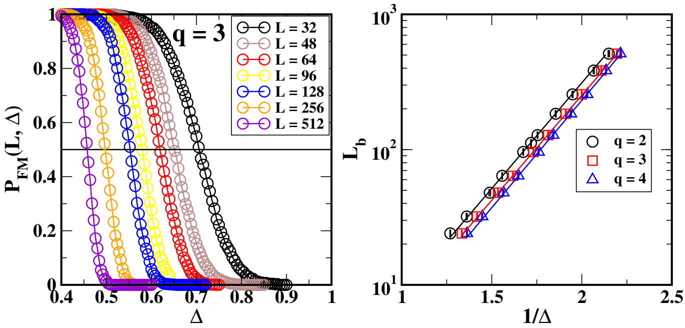

Define L_b as system size such that 50% of disorder samples at given h are FM (Seppälä et al., 1998).

What is the correct form?

$$L_b \sim \exp(A/h) \quad \text{or} \quad \exp(A/h^2)$$

Break-up length (cont'd)

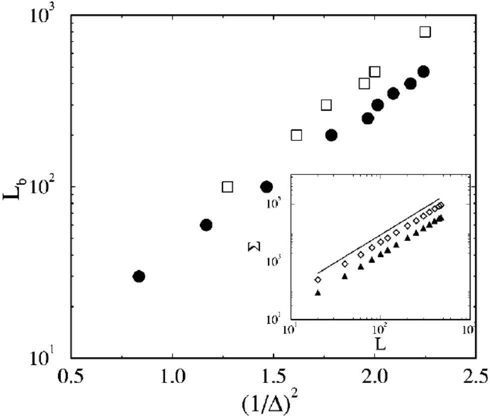

Seppälä et al., 1998

What is the correct form?

$$L_b \sim \exp(A/h^2)$$

Break-up length (cont'd)

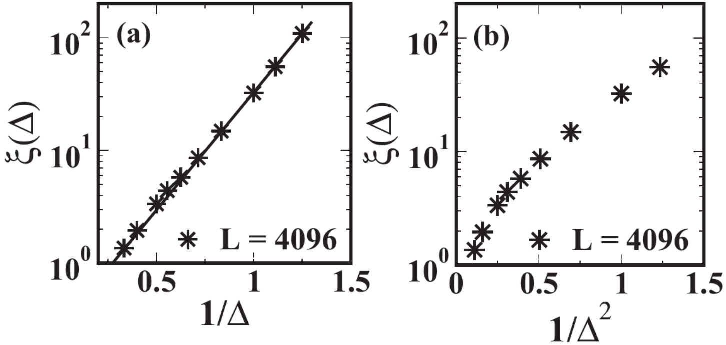

Shrivastav et al. 2014

What is the correct form?

$$L_b \sim \exp(A/h^2) \quad \text{or} \quad \exp(A/h)$$

Maximum flows and graph cuts

Split up Ising model Hamiltonian,

$$-\mathcal{H} = \sum_{\langle ij \rangle} J_{ij}\, s_i s_j = W^+ + W^- - W^\pm = K - 2W^\pm, \tag{1}$$

where $K = \sum_{\langle ij \rangle} J_{ij}$, and

$$W^+ = \sum_{\substack{\langle ij \rangle \\ s_i = s_j = +1}} J_{ij}, \quad W^- = \sum_{\substack{\langle ij \rangle \\ s_i = s_j = -1}} J_{ij}, \quad W^\pm = \sum_{\substack{\langle ij \rangle \\ s_i \neq s_j}} J_{ij} \tag{2}$$

Maximum flows and graph cuts

Split up Ising model Hamiltonian,

$$-\mathcal{H} = \sum_{\langle ij \rangle} J_{ij}\, s_i s_j = W^+ + W^- - W^\pm = K - 2W^\pm, \tag{1}$$

where $K = \sum_{\langle ij \rangle} J_{ij}$, and

$$W^+ = \sum_{\substack{\langle ij \rangle \\ s_i = s_j = +1}} J_{ij}, \quad W^- = \sum_{\substack{\langle ij \rangle \\ s_i = s_j = -1}} J_{ij}, \quad W^\pm = \sum_{\substack{\langle ij \rangle \\ s_i \neq s_j}} J_{ij} \tag{2}$$

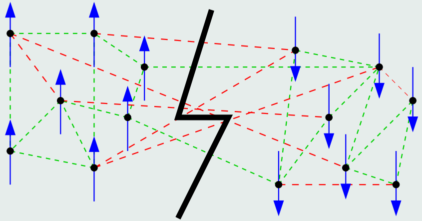

Then, a ground state is given by a configuration with **minimal cut** $W^\pm$, which divides the spins between the "up" and "down" states.

Maximum flows and graph cuts (2)

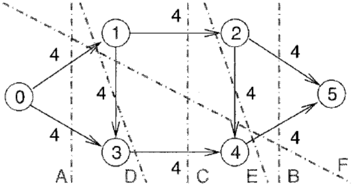

Maximum flows and graph cuts (2)

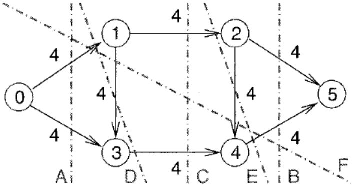

The RFIM can be mapped onto a maximum flow problem (Picard & Ratliff, 1975) where

Maximum flows and graph cuts (2)

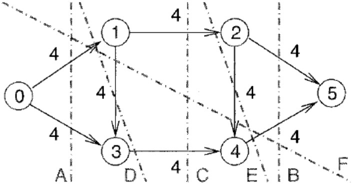

The RFIM can be mapped onto a maximum flow problem (Picard & Ratliff, 1975) where

- all up spins are connected to the source, all down spins are connected to the sink

Maximum flows and graph cuts (2)

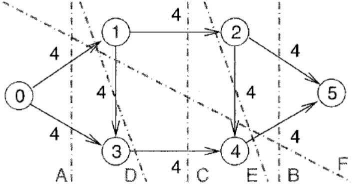

The RFIM can be mapped onto a maximum flow problem (Picard & Ratliff, 1975) where

- all up spins are connected to the source, all down spins are connected to the sink
- a **cut** separates the two classes of sites, the energy of the configuration corresponds to the weight of the cut

Maximum flows and graph cuts (2)

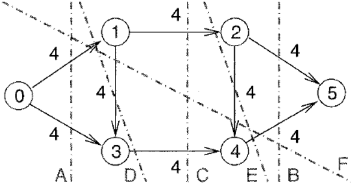

The RFIM can be mapped onto a maximum flow problem (Picard & Ratliff, 1975) where

- all up spins are connected to the source, all down spins are connected to the sink
- a **cut** separates the two classes of sites, the energy of the configuration corresponds to the weight of the cut
- due to the **max-flow–min-cut theorem**, the ground-state (min-cut) configuration occurs for maximum flow through the network

Maximum flows and graph cuts (2)

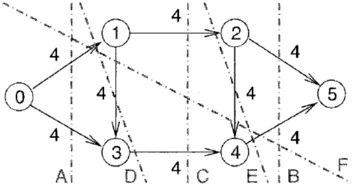

The RFIM can be mapped onto a maximum flow problem (Picard & Ratliff, 1975) where

- all up spins are connected to the source, all down spins are connected to the sink
- a **cut** separates the two classes of sites, the energy of the configuration corresponds to the weight of the cut
- due to the **max-flow–min-cut theorem**, the ground-state (min-cut) configuration occurs for maximum flow through the network
- there are efficient (**polynomial time**) algorithms to solve maximum flow exactly (Ford-Fulkerson, Edmonds-Karp, push relabel, ...)

Numerical study

We use **exact** ground-state algorithms to study the breakup length ℓ_b and the **correlation lengths** ξ and ξ^{dis} for 10^6 samples and lattice sizes $L = 128$, 256, 512, 1024, and 2048.

Numerical study

We use **exact** ground-state algorithms to study the breakup length ℓ_b and the **correlation lengths** ξ and ξ^{dis} for 10^6 samples and lattice sizes $L = 128$, 256, 512, 1024, and 2048.

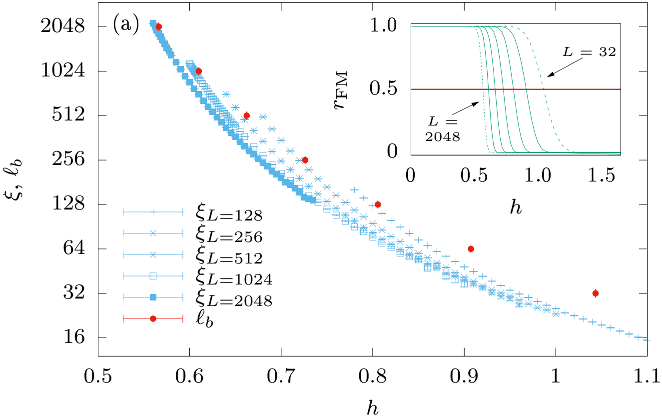

Numerical study

We use **exact** ground-state algorithms to study the breakup length ℓ_b and the **correlation lengths** ξ and ξ^{dis} for 10^6 samples and lattice sizes $L = 128$, 256, 512, 1024, and 2048.

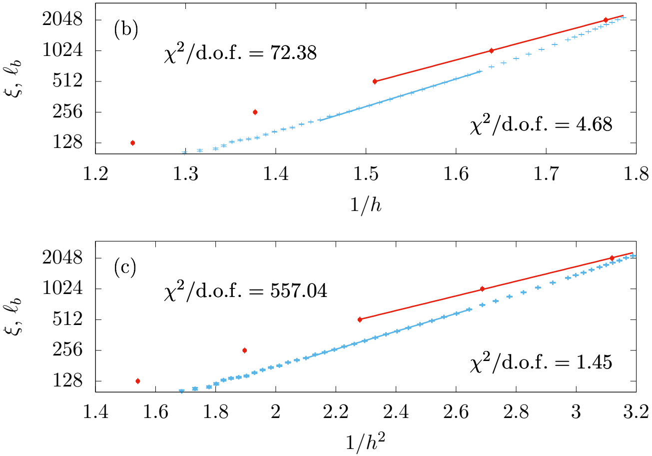

Correlation length: triangular lattice

Strong evidence for $\xi \sim \exp(A/h^2)$ form on the square lattice.

Correlation length: triangular lattice

Strong evidence for $\xi \sim \exp(A/h^2)$ form on the square lattice.

Hayden, Raju and Sethna, 2019: since $w \not\leftrightarrow -w$ on non-bipartite lattices, the RG equation should take the form

$$\mathrm{d}w/\mathrm{d}l = -(\epsilon/2)w + Bw^2 + Aw^3 + \ldots,$$

implying a leading divergence $\xi \sim \exp(A/h)$ for the **triangular** lattice.

Correlation length: triangular lattice

Strong evidence for $\xi \sim \exp(A/h^2)$ form on the square lattice.

Hayden, Raju and Sethna, 2019: since $w \not\leftrightarrow -w$ on non-bipartite lattices, the RG equation should take the form

$$\mathrm{d}w/\mathrm{d}l = -(\epsilon/2)w + Bw^2 + Aw^3 + \ldots,$$

implying a leading divergence $\xi \sim \exp(A/h)$ for the **triangular** lattice.

Is this supported by the data?

Correlation length: comparison

We find clear evidence for $\xi \sim \exp(A/h^2)$ for the connected and disconnected correlation lengths in the square and triangular lattices.

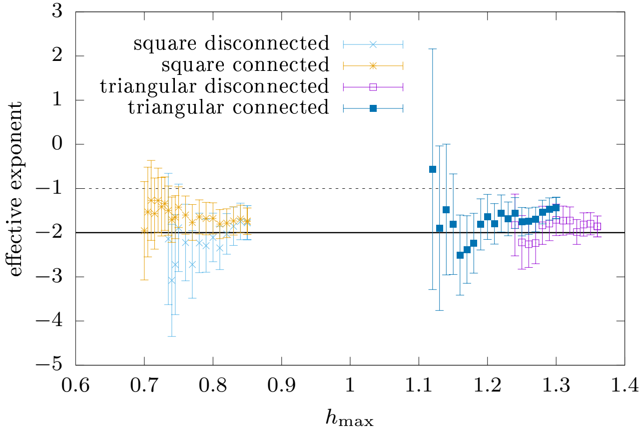

Random-field Potts model

Very little work to date:

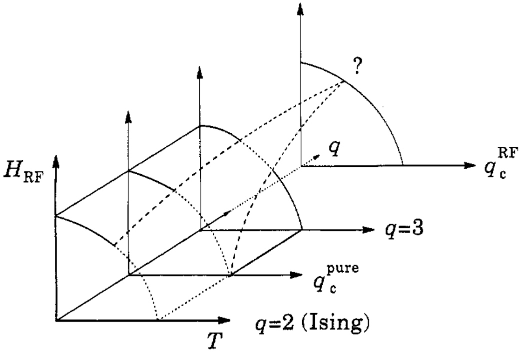

Blankschtein, Shapir, Aharony, 1984

Random-field Potts model

Very little work to date:

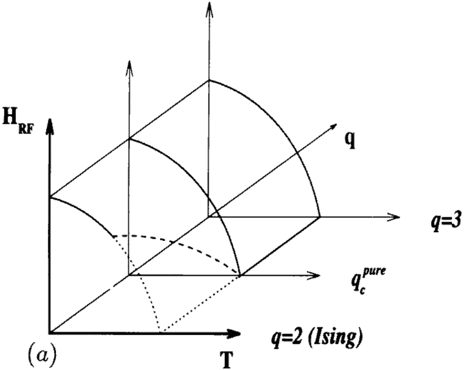

Goldschmidt and Xu, 1985/86

Random-field Potts model

Very little work to date:

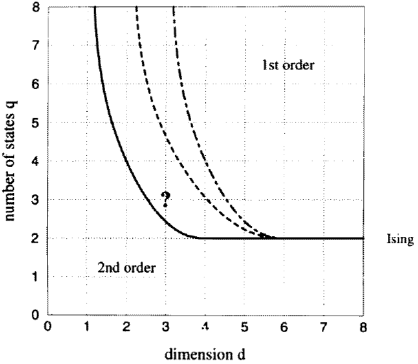

Goldschmidt and Xu, 1985/86

Random-field Potts model

Very little work to date:

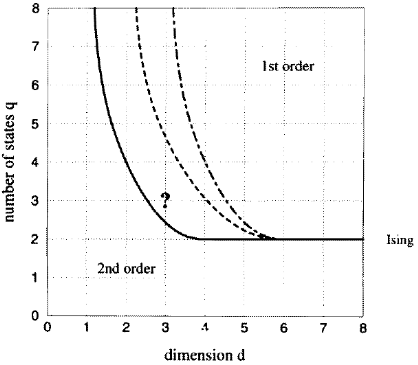

Goldschmidt and Xu, 1985/86

Most recent study by Eichhorn and Binder (1995/96): possible 2nd order transition for 3D $q = 3$ model.

Maximum flows and graph cuts (2)

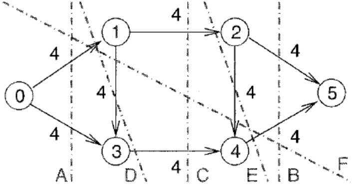

The RFIM can be mapped onto a maximum flow problem (Picard & Ratliff, 1975) where

- all up spins are connected to the source, all down spins are connected to the sink
- a **cut** separates the two classes of sites, the energy of the configuration corresponds to the weight of the cut
- due to the **max-flow–min-cut theorem**, the ground-state (min-cut) configuration occurs for maximum flow through the network
- there are efficient (**polynomial time**) algorithms to solve maximum flow exactly (Ford-Fulkerson, Edmonds-Karp, push relabel, ...)

Graph cuts and the Potts model

We consider the Hamiltonian

$$\mathcal{H} = -J \sum_{\langle ij \rangle} \delta_{s_i,s_j} - \sum_i \sum_{\alpha=0}^{q-1} h_i^\alpha \delta_{s_i,\alpha},$$

Graph cuts and the Potts model

We consider the Hamiltonian

$$\mathcal{H} = -J \sum_{\langle ij \rangle} \delta_{s_i,s_j} - \sum_i \sum_{\alpha=0}^{q-1} h_i^\alpha \delta_{s_i,\alpha},$$

The $q = 2$ case is equivalent to the RFIM,

$$\mathcal{H} = -\frac{J}{2} \sum_{\langle ij \rangle} [\sigma_i \sigma_j + 1] - \frac{1}{2} \sum_i [(h_i^+ - h_i^-)\sigma_i + (h_i^+ + h_i^-)],$$

Graph cuts and the Potts model

We consider the Hamiltonian

$$\mathcal{H} = -J \sum_{\langle ij \rangle} \delta_{s_i,s_j} - \sum_i \sum_{\alpha=0}^{q-1} h_i^\alpha \delta_{s_i,\alpha},$$

The $q = 2$ case is equivalent to the RFIM,

$$\mathcal{H} = -\frac{J}{2} \sum_{\langle ij \rangle} [\sigma_i \sigma_j + 1] - \frac{1}{2} \sum_i [(h_i^+ - h_i^-)\sigma_i + (h_i^+ + h_i^-)],$$

The ground-state problem for $q > 2$ corresponds to a **multi-terminal flow problem** that is **NP hard**.

Graph cuts and the Potts model

We consider the Hamiltonian

$$\mathcal{H} = -J \sum_{\langle ij \rangle} \delta_{s_i,s_j} - \sum_i \sum_{\alpha=0}^{q-1} h_i^\alpha \delta_{s_i,\alpha},$$

The $q = 2$ case is equivalent to the RFIM,

$$\mathcal{H} = -\frac{J}{2} \sum_{\langle ij \rangle} [\sigma_i \sigma_j + 1] - \frac{1}{2} \sum_i [(h_i^+ - h_i^-)\sigma_i + (h_i^+ + h_i^-)],$$

The ground-state problem for $q > 2$ corresponds to a **multi-terminal flow problem** that is **NP hard**.

We need to revert to **approximation methods**.

Approximate graph cuts

Boykov, Veksler and Zabih (2001) propose a method for problems in computer vision:

$$E(\{s_i\}) = \sum_{i,j} V_{ij}(s_i, s_j) + \sum_i D_i(s_i).$$

Approximate graph cuts

Boykov, Veksler and Zabih (2001) propose a method for problems in computer vision:

$$E(\{s_i\}) = \sum_{i,j} V_{ij}(s_i, s_j) + \sum_i D_i(s_i).$$

It is based on solving an effective two-terminal (Ising) problem by freezing some degrees of freedom.

Approximate graph cuts

Boykov, Veksler and Zabih (2001) propose a method for problems in computer vision:

$$E(\{s_i\}) = \sum_{i,j} V_{ij}(s_i, s_j) + \sum_i D_i(s_i).$$

It is based on solving an effective two-terminal (Ising) problem by freezing some degrees of freedom.

- **α-β-swap move**
  picks two labels $\alpha \neq \beta \in \{0, 1, \ldots, q-1\}$ and freeze all labels apart from α and β

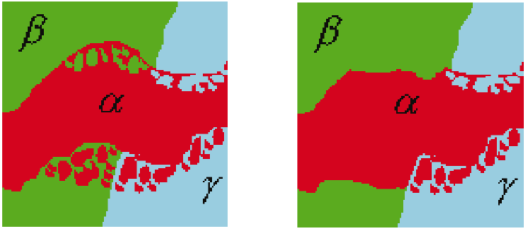

Approximate graph cuts

Boykov, Veksler and Zabih (2001) propose a method for problems in computer vision:

$$E(\{s_i\}) = \sum_{i,j} V_{ij}(s_i, s_j) + \sum_i D_i(s_i).$$

It is based on solving an effective two-terminal (Ising) problem by freezing some degrees of freedom.

- α **expansion move**
  pick and freeze a label α; either keep or flip remaining pixels into α state

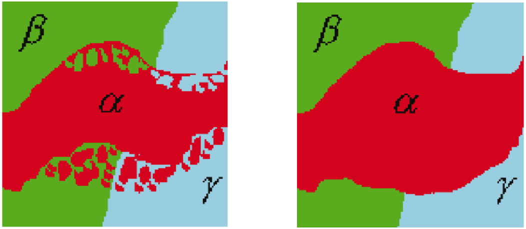

Approximate graph cuts

Boykov, Veksler and Zabih (2001) propose a method for problems in computer vision:

$$E(\{s_i\}) = \sum_{i,j} V_{ij}(s_i, s_j) + \sum_i D_i(s_i).$$

It is based on solving an effective two-terminal (Ising) problem by freezing some degrees of freedom.

- α **expansion move**
  pick and freeze a label α; either keep or flip remaining pixels into α state

Works well in **computer vision** (paper has 10,000 citations!). How about the RFPM?

Results: 3D $q = 3$ RFPM – initial conditions

Use repeated runs to increase success probabilities.

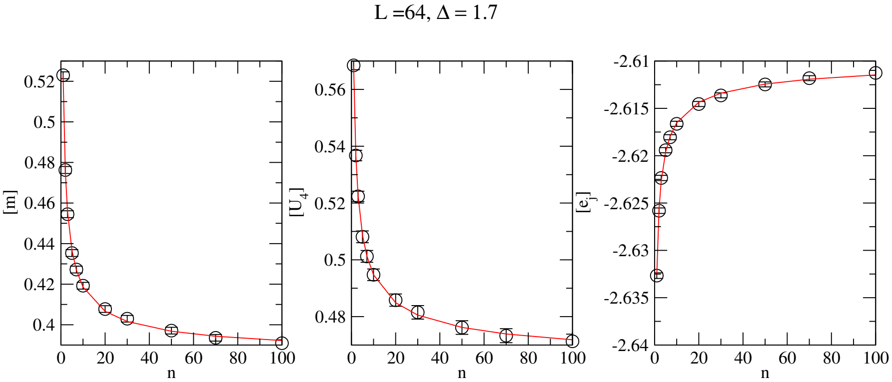

Results: 3D $q = 3$ RFPM – initial conditions

Use repeated runs to increase success probabilities.

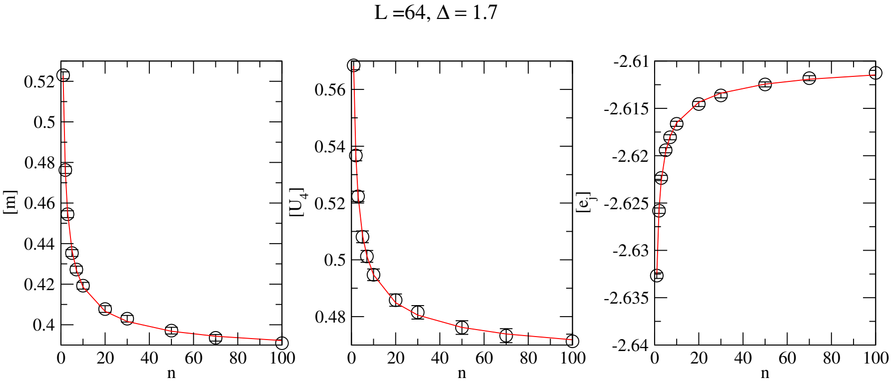

Quantities converge in power laws:

$$\mathcal{O}(n) = an^{-b}(1 + cn^{-e}) + \mathcal{O}^*.$$

Results: 3D $q = 3$ RFPM – magnetization

Sample thermodynamic quantities either for $n = 100$ or extrapolate.

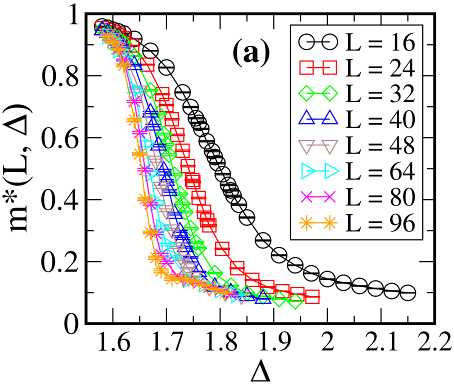

Results: 3D $q = 3$ RFPM – magnetization

Sample thermodynamic quantities either for $n = 100$ or extrapolate.

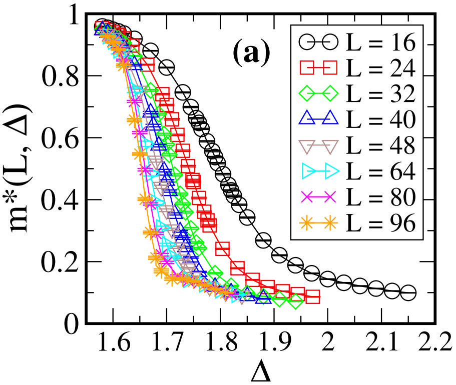

Scaling form of the magnetization:

$$m^*(\Delta, L) = L^{-\beta/\nu} \widetilde{\mathcal{M}} \left[(\Delta - \Delta_c) L^{1/\nu} \right],$$

Results: 3D $q = 3$ RFPM – magnetization

Sample thermodynamic quantities either for $n = 100$ or extrapolate.

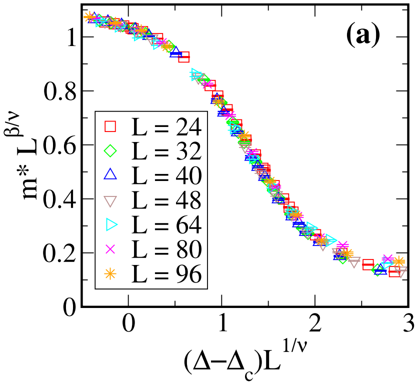

Scaling form of the magnetization:

$$m^*(\Delta, L) = L^{-\beta/\nu} \widetilde{\mathcal{M}} \left[(\Delta - \Delta_c) L^{1/\nu} \right],$$

Results: 3D $q = 3$ RFPM — magnetization

Sample thermodynamic quantities either for $n = 100$ or extrapolate.

n	Δ_c	$1/\nu$	β/ν	$\bar{\gamma}/\nu$	S_1	S_2
1	1.636(2)	0.837(9)	0.0460(9)	2.9084(14)	2.30	2.38
5	1.626(3)	0.812(6)	0.0403(8)	2.9220(15)	1.82	1.69
10	1.623(5)	0.828(15)	0.0387(7)	2.9230(15)	1.28	1.58
50	1.617(4)	0.797(4)	0.0340(8)	2.9323(16)	1.25	1.38
100	1.616(1)	0.774(6)	0.0330(10)	2.9337(15)	1.20	1.36
∞	1.606(3)	0.723(4)	0.0306(23)	2.9402(30)	0.82	0.87

Table: A summary of exponents from the FSS of the $m(L, \Delta, n)$ for finite as well as infinite n. The numbers in the parenthesis denote the error bars in the last significant digit.

Scaling form of the magnetization:

$$m^*(\Delta, L) = L^{-\beta/\nu} \widetilde{\mathcal{M}} \left[(\Delta - \Delta_c) L^{1/\nu} \right],$$

Results: 3D $q = 3$ RFPM – specific heat

No direct access to fluctuations in ground states. Hence consider

$$C(\Delta) = \frac{\partial [e_J(\Delta)]}{\partial \Delta}.$$

Results: 3D $q = 3$ RFPM — specific heat

No direct access to fluctuations in ground states. Hence consider

$$C(\Delta) = \frac{\partial [e_J(\Delta)]}{\partial \Delta}.$$

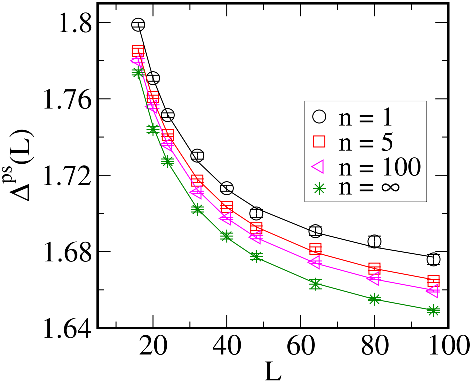

Results: 3D $q = 3$ RFPM — specific heat

No direct access to fluctuations in ground states. Hence consider

$$C(\Delta) = \frac{\partial[e_J(\Delta)]}{\partial\Delta}.$$

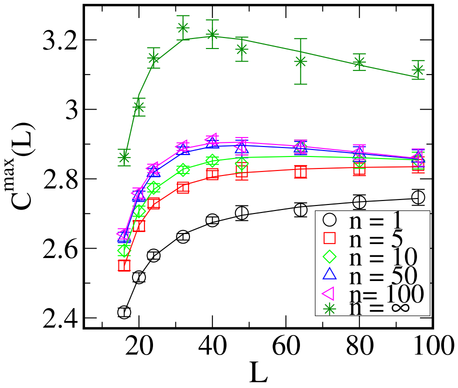

Results: 3D $q = 3$ RFPM — specific heat

No direct access to fluctuations in ground states. Hence consider

$$C(\Delta) = \frac{\partial [e_J(\Delta)]}{\partial \Delta}.$$

n	Δ_c	$1/\nu$	α/ν	ω	Q_1	Q_2
1	1.644(6)	0.850(70)	$0.023(12)$	$2.67(87)$	0.74	0.71
5	1.626(3)	0.774(32)	$-0.002(11)$	$2.62(68)$	0.32	0.70
10	1.621(3)	0.767(25)	$-0.019(13)$	$2.39(61)$	0.14	0.52
50	1.620(2)	0.776(21)	$-0.046(20)$	$1.87(53)$	0.12	0.50
100	1.620(2)	0.780(21)	$-0.049(20)$	$1.86(52)$	0.15	0.49
∞	1.611(4)	0.733(28)	$-0.059(20)$	$2.52(73)$	0.14	0.93

Table: A summary of exponents from the fits of the peak positions $\Delta^{\mathrm{ps}}(L, n)$ and the heights of the specific heat $C^{\max}(L, n)$. Q_1 is the quality of the fit for the data of $\Delta^{\mathrm{ps}}(L, n)$, and Q_2 is the quality of the fit for the data of $C^{\max}(L, n)$. The numbers in the parenthesis denote the error bars in the last significant digits.

$$C^{\max}(L) = C_0 + aL^{\alpha/\nu}(1 + bL^{-\omega}).$$

Results: 3D $q = 3$ RFPM — susceptibility

We cannot make use of a fluctuation-dissipation relation as the ground state is unique (for continuous fields). Hence we could rely on

$$\chi^{\mu}(\Delta) = \left[\frac{\partial M^{\mu}(\{h_i^{\alpha}\}, H)}{\partial H}\right]_{H=0}.$$

Results: 3D $q = 3$ RFPM — susceptibility

We cannot make use of a fluctuation-dissipation relation as the ground state is unique (for continuous fields). Hence we could rely on

$$\chi^\mu(\Delta) = \left[\frac{\partial M^\mu(\{h_i^\alpha\}, H)}{\partial H}\right]_{H=0}.$$

This requires ground-state calculations at a number of different field strengths (numerical differentiation). It does not work for non-exact methods.

Results: 3D $q = 3$ RFPM — susceptibility

We cannot make use of a fluctuation-dissipation relation as the ground state is unique (for continuous fields). Hence we could rely on

$$\chi^\mu(\Delta) = \left[\frac{\partial M^\mu(\{h_i^\alpha\}, H)}{\partial H}\right]_{H=0}.$$

This requires ground-state calculations at a number of different field strengths (numerical differentiation). It does not work for non-exact methods.

Instead, explicitly integrate the effect of the shift in the coupling distribution (Schwartz and Soffer, 1985), leading to

$$\chi^\beta = \lim_{H^\beta \to 0} \frac{1}{N} \left[\frac{\partial \langle M^\beta \rangle}{\partial H^\beta}\right]_{\text{av}} = \frac{1}{\Delta^2} \left[\langle m^\beta \rangle \sum_i h_i^\beta\right]_{\text{av}},$$

Results: 3D $q = 3$ RFPM — susceptibility

We cannot make use of a fluctuation-dissipation relation as the ground state is unique (for continuous fields). Hence we could rely on

$$\chi^\mu(\Delta) = \left[\frac{\partial M^\mu(\{h_i^\alpha\}, H)}{\partial H}\right]_{H=0}.$$

This requires ground-state calculations at a number of different field strengths (numerical differentiation). It does not work for non-exact methods.

Instead, explicitly integrate the effect of the shift in the coupling distribution (Schwartz and Soffer, 1985), leading to

$$\chi^\beta = \lim_{H^\beta \to 0} \frac{1}{N}\left[\frac{\partial \langle M^\beta \rangle}{\partial H^\beta}\right]_{\mathrm{av}} = \frac{1}{\Delta^2}\left[\langle m^\beta \rangle \sum_i h_i^\beta\right]_{\mathrm{av}},$$

Without explicitly breaking the symmetry, however, there is no peak in this χ. Scaling arguments imply that one should use a field $H \sim L^{3/2}$.

Results: 3D $q = 3$ RFPM – susceptibility

Use repeated runs to increase success probabilities.

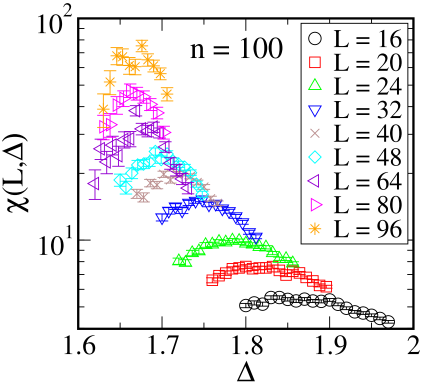

Results: 3D $q = 3$ RFPM – susceptibility

Use repeated runs to increase success probabilities.

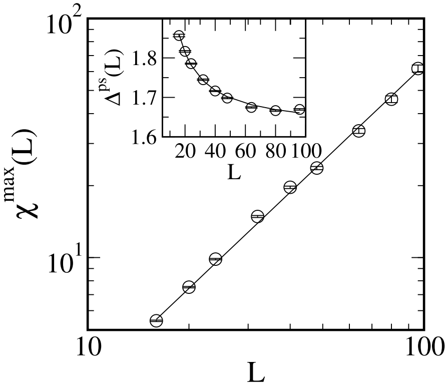

Consider the scaling form

$$\chi(L, \Delta) = L^{\gamma/\nu} \widetilde{\chi} \left[(\Delta - \Delta_c) L^{1/\nu} \right].$$

Results: 3D $q = 3$ RFPM — exponents

In summary, we have the following estimates:

	RFIM	$q = 3$ RFPM
ν	1.38(10)	1.383(8)
α	-0.16(35)	-0.082(28)
β	0.019(4)	0.0423(32)
γ	2.05(15)	2.089(84)
η	0.5139(9)	0.49(6)
$\bar{\eta}$	1.028(2)	1.060(3)
θ	1.487(1)	1.43(6)
$\alpha + 2\beta + \gamma$	2.00(31)	2.08(9)

Results: 3D $q = 3$ RFPM — exponents

In summary, we have the following estimates:

	RFIM	$q = 3$ RFPM
ν	1.38(10)	1.383(8)
α	-0.16(35)	-0.082(28)
β	0.019(4)	0.0423(32)
γ	2.05(15)	2.089(84)
η	0.5139(9)	0.49(6)
$\bar{\eta}$	1.028(2)	1.060(3)
θ	1.487(1)	1.43(6)
$\alpha + 2\beta + \gamma$	2.00(31)	2.08(9)

Consider Rushbrooke's law:

$$\alpha + 2\beta + \gamma = 2.$$

Results: 3D $q = 3$ RFPM – exponents

In summary, we have the following estimates:

	RFIM	$q = 3$ RFPM
ν	1.38(10)	1.383(8)
α	-0.16(35)	-0.082(28)
β	0.019(4)	0.0423(32)
γ	2.05(15)	2.089(84)
η	0.5139(9)	0.49(6)
$\bar{\eta}$	1.028(2)	1.060(3)
θ	1.487(1)	1.43(6)
$\alpha + 2\beta + \gamma$	2.00(31)	2.08(9)

Consider Rushbrooke's law:

$$\alpha + 2\beta + \gamma = 2.$$

RFIM:

$$\alpha + 2\beta + \gamma = 2.00(31).$$

Results: 3D $q = 3$ RFPM — exponents

In summary, we have the following estimates:

	RFIM	$q = 3$ RFPM
ν	1.38(10)	1.383(8)
α	-0.16(35)	-0.082(28)
β	0.019(4)	0.0423(32)
γ	2.05(15)	2.089(84)
η	0.5139(9)	0.49(6)
$\bar{\eta}$	1.028(2)	1.060(3)
θ	1.487(1)	1.43(6)
$\alpha + 2\beta + \gamma$	2.00(31)	2.08(9)

Consider Rushbrooke's law:

$$\alpha + 2\beta + \gamma = 2.$$

RFIM:

$$\alpha + 2\beta + \gamma = 2.00(31).$$

RFPM:

$$\alpha + 2\beta + \gamma = 2.08(9).$$

Conclusions

- hard optimization problems are ubiquitous in statistical mechanics problems
- for the hardest problems, general-purpose techniques are not sufficient
- use results from combinatorial problems for non-combinatorial ones

Conclusions

- hard optimization problems are ubiquitous in statistical mechanics problems
- for the hardest problems, general-purpose techniques are not sufficient
- use results from combinatorial problems for non-combinatorial ones

2D spin glass:

- new mapping allows to treat huge systems up to $10\,000 \times 10\,000$ spins
- strong scaling corrections in frustrated systems
- connection to stochastic Loewner evolution

Conclusions

- hard optimization problems are ubiquitous in statistical mechanics problems
- for the hardest problems, general-purpose techniques are not sufficient
- use results from combinatorial problems for non-combinatorial ones

2D RFIM:

- clear evidence for $\sim \exp(A/h^2)$ scaling predicted by Binder
- no violation of universality for different lattice structures
- complete lack of self-averaging of the correlation length

Conclusions

- hard optimization problems are ubiquitous in statistical mechanics problems
- for the hardest problems, general-purpose techniques are not sufficient
- use results from combinatorial problems for non-combinatorial ones

3D $q = 3$ RFPM:

- approximate ground states from graph cuts and α expansion
- systematic extrapolation to $n \to \infty$
- critical exponents close to, but potentially different from 3D RFIM
- two-exponent scaling, $\overline{\gamma}/\nu = 2.904(30) \approx 2\gamma/\nu = 3.02(12)$
- hyperscaling violation, $(d - \theta)\nu = 2.17(8) \approx 2 - \alpha = 2.08(10)$ with $\theta = 1.43(6)$

Acknowledgements

References

[1] M. Kumar and M. Weigel, Quasi-exact ground-state algorithm for the random-field Potts model, Preprint arXiv:2204.11745.

[2] M. Kumar, V. Banerjee, S. Puri, and M. Weigel, Critical behavior of the three-state random-field Potts model in three dimensions, Phys. Rev. Res. 4, L042041 (2022).

[3] M. Kumar and M. Weigel, On the comparison of optimization algorithms for the random-field Potts model, J. Phys.: Conf. Ser. 2241, 012003 (2022).

[4] R. Kumar, J. Gross, W. Janke, and M. Weigel, Massively parallel simulations for disordered systems, Eur. Phys. J. B 93, 79 (2020).

[5] H. Khoshbakht and M. Weigel, Domain-wall excitations in the two-dimensional Ising spin glass, Phys. Rev. B 97, 064410 (2018).

Acknowledgements

References

[1] M. Kumar and M. Weigel, Quasi-exact ground-state algorithm for the random-field Potts model, Preprint arXiv:2204.11745.

[2] M. Kumar, V. Banerjee, S. Puri, and M. Weigel, Critical behavior of the three-state random-field Potts model in three dimensions, Phys. Rev. Res. 4, L042041 (2022).

[3] M. Kumar and M. Weigel, On the comparison of optimization algorithms for the random-field Potts model, J. Phys.: Conf. Ser. 2241, 012003 (2022).

[4] R. Kumar, J. Gross, W. Janke, and M. Weigel, Massively parallel simulations for disordered systems, Eur. Phys. J. B 93, 79 (2020).

[5] H. Khoshbakht and M. Weigel, Domain-wall excitations in the two-dimensional Ising spin glass, Phys. Rev. B 97, 064410 (2018).

You

Thank you for your attention!